prevents communication between the fibers (*11*). However, we found that at the metathoracic ganglion the axon gives off several neurites which ramify in the neuropil. In several series (three preparations) of serial sections through the metathoracic ganglion, we found that the branches from two different giant interneurons come into close proximity (Fig. 2E) (*12*). In this area the distance between the giant interneurons' neurite membranes is only 7 to 10 nm (Fig. 2F). We have observed up to three such regions between two branches (*9*).

That K^+ has an important role in neuronal interaction has been demonstrated before (*13*). In most of these studies the increase in extracellular K^+ concentration was either due to stimulation of a single neuron at high frequency or the combined action of a group of neurons; furthermore, a fraction of adjacent neuronal elements in the vicinity of the stimulated pathway were affected, whereas others were not. In the present report we demonstrate a specific and efficient interaction in which a single action potential is capable of generating a significant depolarization in a single adjacent neuron. We propose that this depolarization is due to an increase in K^+ concentration at a defined and restricted region. Our results cannot be explained by the presence of either chemical or electrotonic synapses and are consistent with the proposed hypothesis.

Y. YAROM
M. E. SPIRA

Neurobiology Unit, Life Sciences Institute, Hebrew University, Jerusalem, Israel

References and Notes

1. M. V. L. Bennett, in *Handbook of Physiology—The Nervous System*, E. Kandel, Ed. (Williams & Wilkins, 1977), vol. 1, pp. 357–416.
2. M. E. Spira, Y. Yarom, I. Parnas, *J. Neurophysiol.* **39**, 882 (1976).
3. For these experiments we used late nymphal stages of *P. americana*. At these stages chemically mediated synaptic inputs with a rise time of 2.8 msec and a reversal potential range between −65 and −57 mV can be activated by stimulation of seven different nerves connected to the metathoracic ganglion (M. E. Spira and Y. Yarom, unpublished observations). The nerve cord was isolated as described (*2*). The isolated nerve cord was continuously perfused by physiological solution containing 214 m*M* NaCl, 3.1 m*M* KCl, 7 m*M* $CaCl_2$, and 1 m*M* tris. The *p*H was adjusted to 7.2 to 7.4.
4. The relation between GGSP amplitude and membrane potential (Fig. 1C) extrapolates to an apparent reversal potential ranging from −10 to 0 mV. This result is expected if the GGSP arises from an increase in the extracellular K^+ concentration [P. Rudomin, E. Stefani, R. Werman, *J. Neurophysiol.* **42**, 912 (1979)].
5. Addition of 5 m*M* $CoCl_2$ to the physiological solution slightly decreased the time constant of the membrane. Therefore, at least part of the observed increase in the rate of decay of the GGSP can be attributed to the direct effect of the cobalt ions on the membrane properties of the giant interneuron.
6. C. M. Armstrong, *J. Gen. Physiol.* **54**, 553 (1963); B. Hille, *ibid.* **50**, 1287 (1967); R. Werman, F. V. McCann, H. Grundfest, *ibid.* **44**, 979 (1961).
7. Y. A. Cottrell and J. B. Macon, *J. Physiol. (London)* **236**, 435 (1974); M. Deschenes and M. V. L. Bennett, *Brain Res.* **77**, 169 (1974); J. S. Kehoe, *J. Physiol. (London)* **225**, 147 (1972); K. Kusano, D. R. Livengood, R. Werman, *J. Gen. Physiol.* **50**, 2519 (1967); D. Paupardin-Tritsch and H. M. Gershenfeld, *Brain Res.* **58**, 524 (1973).
8. The electrode was filled with 1*M* tetraethylammonium chloride; its resistance was about 200 megohms. To inject the TEA we used 0.5-msec, 200-nA positive square pulses delivered from a constant current source.
9. Assuming that a single action potential in a giant interneuron produces an efflux of 4×10^{-12} mole of potassium ions per square centimeter [A. L. Hodgkin, *The Conduction of the Nervous Impulse* (Thomas, Springfield, Ill., 1964), pp. 42–44] and taking into account the extracellular space between the closely apposed interneuron branches and the membrane properties, we calculate that a single action potential in one giant interneuron would evoke a 1-mV depolarizing potential in the other, provided the radius of the closely apposed membranes is 10 μm, or 16 junctions with radii of 2.5 μm form between the interneurons. In our ultrastructural study we have observed up to three regions of close membrane apposition between two branches. Each of the giant interneurons studied emits up to seven branches (Y. Yarom and M. E. Spira, in preparation). Thus, if each branch makes up two to three such junctions the total area of membrane in close apposition will be about that estimated by our calculations.
10. M. Castel, M. E. Spira, I. Parnas, Y. Yarom, *J. Neurophysiol.* **39**, 900 (1976); N. H. Lane, in *Insect Neurobiology*, J. E. Threherne, Ed. (North-Holland, Amsterdam, 1974), pp. 1–61.
11. Y. Grossman and M. J. Gutnick, *Brain Res.* **211**, 196 (1981).
12. The two branches shown in Fig. 2E are from giant interneurons II (Ax.b.II) and III (Ax.b.III). Nomenclature after C. L. Harris and T. Smyth, *Comp. Biochem Physiol.* **40**, 295 (1971).
13. D. L. Alkon and Y. Grossman, *J. Neurophysiol.* **42**, 640 (1978); D. H. Barron and B. H. C. Matthews, *J. Physiol. (London)* **92**, 276 (1932); B. A. Baylor and J. G. Nicholls, *ibid.* **203**, 555 (1969); J. G. Eccles, R. Magni, W. D. Willis, *ibid.* **160**, 62 (1962); S. D. Erulkar and F. F. Weight, *ibid.* **266**, 209 (1977); K. Krnjevic and M. E. Morris, *Can. J. Physiol. Pharmacol.* **50**, 1214 (1972); C. Nicholson, in *The Neurosciences, Fourth Study Program* (MIT Press, Cambridge, Mass., 1979), pp. 457–477; P. Rudomin, R. B. Leonard, E. D. Willis, *J. Neurophysiol.* **44**, 126 (1978); N. C. Spitzer, *J. Physiol. (London)* **155**, 105 (1976).
14. We thank I. Parnas for discussions and support, R. Werman for helpful comments, and A. Dormann for technical assistance. This work was supported by grants from the United States–Israel Binational Science Foundation (No. 1829 and No. 1534) to the laboratories of M.E.S. and I. Parnas. Y.Y. is a Batsheva Scholar.

17 July 1981; revised 16 October 1981

A Virally Induced Obesity Syndrome in Mice

Abstract. *An obesity syndrome was found in a number of mice infected as young adults with canine distemper virus, a morbillivirus antigenically related to measles. Body weights of obese animals 16 to 20 weeks after infection were comparable to those reported for genetically obese mice and for mice rendered obese by hypothalamic lesions. The total number of adipocytes in specific fat deposits was greater in obese animals than in their lean littermates. This hyperplasia was accompanied by moderate cell enlargement. Pancreatic islet tissue was also hypercellular in the obese mice. Brain tissue from the obese mice showed no overt pathology, and immunofluorescence staining for viral antigens was negative. There may be a selective, virus-induced disruption of critical brain catecholamine pathways.*

During an investigation of the pathological consequences of canine distemper virus infection of the mouse central nervous system, we found that an obesity syndrome developed in a number of animals surviving the infection. To our knowledge, an infectious process has not been considered a possible etiological factor in the pathogenesis of obesity. Experimental models of obesity have fallen into three classes: hypothalamic obesity, produced by electrolytic, chemical, or knife injury to the hypothalamus or to fibers leading to and from the hypothalamus; dietary obesity; and genetically transmitted obesity. Strain-dependent differences in the phenotypic expression of obesity have been noted, for example, at the level of adipose tissue morphology (*1*). Thus, in certain

Table 1. Outcome of canine distemper virus infection in NCS/R mice. Abbreviations: CNS, central nervous system; CDV, canine distemper virus.

Inoculum	*N*	Acute encephalitis*	CNS disease 4 to 24 weeks after infection	Obesity 6 to 20 weeks after infection	No CNS disease, no obesity
CDV (10^3 PFU, intracerebrally)	120	52	14	18	36
CDV (5×10^4 PFU, intraperitoneally)	12			2	10
Normal suckling mouse brain suspension (intracerebrally)	35				35
HBSS (intracerebrally)	45				45

*Animals dead or dying 2 weeks after inoculation.

0036-8075/82/0402-0082$01.00/0

mouse strains, adiposity in the adult animal appears to result from a marked hypertrophy of adipocytes, while in other strains, notably the *ob/ob* strain and the Zucker *fa/fa* rat, adiposity appears to result from both hypertrophy and hyperplasia of adipocytes.

Since the distemper virus experiments indicated a seemingly novel mechanism for the induction of obesity, a study of the phenomenon was carried out focusing on the morphological characteristics of the adipose tissue. Brain tissue was examined to determine the presence or absence of overt pathology. The pancreas, pituitary, and adrenal glands were similarly examined.

Swiss albino mice (NCS/R) were selected for the study. These animals normally are lean; spontaneous obesity has never been encountered among the adults. They were fed unlimited Purina Lab Chow in a temperature-controlled room with a 12-hour light-dark cycle.

Animals 4 to 5 weeks old and weighing 20 g were lightly anesthetized with diethyl ether and injected with approximately 10^3 plaque-forming units (PFU) of canine distemper virus into the left cerebral hemisphere. We used the Onderstepoorte strain of this virus, neuroadapted by serial intracerebral passage in suckling NCS mice (*2*). Stock virus in a 10 percent suspension of suckling mouse brain maintained at −70°C was diluted 1:50 with Hanks balanced salt solution (HBSS) before injection. Groups of control animals were injected with suspensions of normal suckling mouse brain similarly diluted with HBSS or with HBSS alone. A further group of animals was injected intraperitoneally with 5×10^4 PFU of virus.

Obese animals at or near their weight plateau and lean littermates were bled by left ventricular puncture under ether anesthesia and perfused with 10 percent Formalin containing phosphate-buffered saline (*p*H 7.2). For determination of viral antigens in brain by immunofluorescence, perfusion with Formalin was omitted and dissected brain was fixed in 95 percent ethanol. Virus neutralization assays for serum antibodies were performed on Vero cell monolayers grown in microtiter plates. The antibody dilution at which 50 percent of viral plaques were neutralized was determined after 4 days of incubation. Brain, pituitary, kidneys, liver, spleen, pancreas, adrenals, and reproductive organs were dissected free, weighed, and fixed. Pituitary, adrenals, and pancreas were examined histologically. Inguinal, gonadal, and retroperitoneal fat pads were excised and weighed, and the cellularity of these deposits was then determined (*3*).

Table 2. Characteristics of adipose tissue in lean mice and mice with virus-induced obesity. Values are means ± standard errors.

Group	Body weight (g)	Inguinal pad			Gonadal pad			Retroperitoneal pad		
		Wet weight (g)	Cell size (μg lipid/cell)	Cell number (× 10^6)	Wet weight (g)	Cell size (μg lipid/cell)	Cell number (× 10^6)	Wet weight (g)	Cell size (μg lipid/cell)	Cell number (× 10^6)
Obese females ($N = 6$)	52.3 ± 2.5*	1.285 ± 0.215*	0.419 ± 0.042*	2.44 ± 0.27†	6.54 ± 1.25*	0.582 ± 0.087†	9.96 ± 1.13†	1.300 ± 0.170*	0.493 ± 0.047*	2.24 ± 0.26†
Lean females ($N = 4$)	31.8 ± 0.5	0.453 ± 0.048	0.184 ± 0.020	1.73 ± 0.09	1.25 ± 0.19	0.270 ± 0.078	4.73 ± 1.56	0.285 ± 0.035	0.241 ± 0.031	1.12 ± 0.32
Obese males ($N = 3$)	68.3 ± 7.8*	1.950 ± 0.714†	0.465 ± 0.099†	3.33 ± 0.65†	4.99 ± 1.06†	0.625 ± 0.064*	7.19 ± 1.76†	1.860 ± 0.532†	0.395 ± 0.065	3.83 ± 0.48*
Lean males ($N = 4$)	41.1 ± 2.5	0.385 ± 0.060	0.151 ± 0.039	1.90 ± 0.25	1.07 ± 0.18	0.319 ± 0.045	2.92 ± 0.20	0.523 ± 0.119	0.288 ± 0.078	1.49 ± 0.24

*Significantly different from corresponding value for lean mice at $P < .01$ (Student's *t*-test). †$P < .05$.

We have described the development of acute and chronic encephalomyelitis in a number of mice surviving the effects of infection with canine distemper virus (*2*). All the infected animals initially displayed hyperactivity. Histopathological examination of animals with the acute form of the disease revealed encephalitic lesions primarily in the diencephalon (especially around the third ventricle) but also in the cortex and adjacent white matter, hippocampus, brainstem, spinal cords, anterior horns, and—rarely—cerebellar white matter. Mononuclear cell meningitis was most prominent at the base of the brain. The pathological changes in animals less acutely afflicted were similar but less severe.

Obesity (Fig. 1) developed in some mice as early as 6 weeks after infection; it was more commonly observed after 8 to 10 weeks, with animals reaching a weight plateau after 16 to 20 weeks (Fig. 2). The mean body weight of obese animals (63.7 ± 1.5 g) was nearly twice that of lean littermates 33.1 ± 0.8 g. This level of obesity is comparable to that observed in NCS/R mice injected with gold thioglucose and in *ob/ob* mice.

Approximately 26 percent of the animals that did not develop acute central nervous system disease became obese (Table 1). Obesity was not observed among animals inoculated intracerebrally with normal suckling mouse brain extracts or with isotonic salt solution. In one experiment, of 14 animals inoculated intraperitoneally, two were obese 12 to 16 weeks later (Table 1). Obesity developed in male and female animals with equal frequency.

In contrast to the histological findings associated with the encephalitis, hematoxylin- and eosin-stained sections of brain and spinal cord from ten obese and eight infected lean controls were unremarkable, except for the presence of some perivascular mononuclear cell infiltrates in brain sections from one obese animal.

Cresyl violet staining of brain specimens dissected and sectioned to display ventromedial and contiguous hypothalamic nuclei did not reveal differences between obese and lean mice; other brain areas were similarly unremarkable. Immunofluorescence staining for the presence of viral antigens in sections of hypothalamus and other brain areas of obese and lean littermates was negative. Our previous study (*2*) indicated an absence of infectious virus in the brains of animals surviving acute encephalitis.

Table 3. Organ weights for lean mice and mice with virus-induced obesity. Values are means ± standard errors.

Group	Brain (mg)	Liver (g)	Kidneys (mg)	Adrenals (mg)	Spleen (mg)	Pancreas (mg)	Reproductive organs (mg)	Reproductive organs (mg)
							Ovaries	*Uterus*
Obese females (N = 6)	406 ± 27*	2.17 ± 0.17*	552 ± 20*	21.20 ± 7.60	155 ± 27	610 ± 68*	8.56 ± 2.55†	224 ± 52†
Lean females (N = 4)	488 ± 12	1.40 ± 0.10	415 ± 16	8.57 ± 0.79	119 ± 16	407 ± 14	15.7 ± 4.4	352 ± 22
							Testes	*Prostate*
Obese males (N = 3)	420 ± 10	3.68 ± 0.67	1060 ± 50	8.97 ± 3.12	171 ± 16	627 ± 81	254 ± 22	28.7 ± 7.7
Lean males (N = 4)	584 ± 74	2.64 ± 0.32	950 ± 100	11.05 ± 1.07	168 ± 24	536 ± 71	282 ± 22	69.6 ± 10.9†

*Significantly different from corresponding value for lean mice at $P < .01$. †$P < .05$.

Five obese and five lean littermates were found to have neutralizing antibodies to canine dog virus in serum (mean titers, 128 and 64 for obese and lean mice, respectively).

Table 2 presents data on fat pad wet weight, cell size, and cell number for six obese and four infected lean female controls and three obese and four infected lean male controls. Obese animals exhibited higher values than lean animals for all three parameters in the three types of deposits examined. With one exception, all the differences were significant. Also, there were significant differences in organ weights between obese and lean females (Table 3). The brain, ovaries, and uterus weighed less in the obese animals, and the liver, kidneys, and pancreas weighed more. Organ weights were not significantly different between obese and lean males, except for prostate weight, which was lower in the obese mice.

Pancreatic islets in four of six obese animals were larger than normal, appeared to be more numerous, and were hypercellular in both males and females (Fig. 3). In two animals of intermediate weight, similar changes were found to a milder degree. The adrenals and pituitaries were unremarkable.

Canine distemper virus antigenically is closely related to measles virus, being classified with the latter and rinderpest virus of cattle in the morbillivirus subgroup of paramyxoviruses (*4*). Canine distemper virus was used in the present experiments because of its ready adaptation to mice and its capacity to produce central nervous system disease in adults. The development of an obesity syndrome was unexpected. Since obesity was produced by intraperitoneal injection of virus, but did not develop in control animals injected with HBSS or normal suckling mouse brain extracts, virus infection is strongly implicated in the etiology of the syndrome.

The pronounced hyperplasia and moderate hypertrophy of adipose cells in mice with virus-induced obesity are reminiscent of the mature cellularity profile seen in most other obese rats and mice (*5*, *6*). Earlier stages in the development of obesity are usually characterized by extreme adipocyte hypertrophy and little or no hyperplasia (*5*, *7*). The reduced brain, ovary, uterus, and prostate weights found in the mice with virus-induced obesity are characteristic of *ob/ob* mice and *fa/fa* rats, as are increased liver, kidney, and pancreas weights. The *fa/fa* rat and *ob/ob* mouse also typically have enlarged adrenals, but this difference was not found in the mice with virus-induced obesity. Enlarged pancreatic islet tissue, such as that found in the present study, is a consistent feature of all types of obesity in rodents.

No overt abnormalities were observed in brain tissue from the obese animals.

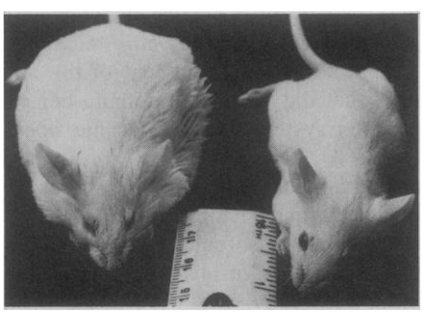

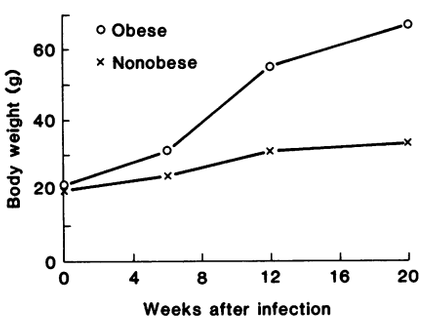

Fig. 1 (left). Mouse with virus-induced obesity and lean littermate. Fig. 2 (right). Change in body weight in female mice as a function of time after intracerebral inoculation with 10^3 PFU of virus. Data points are means for three animals.

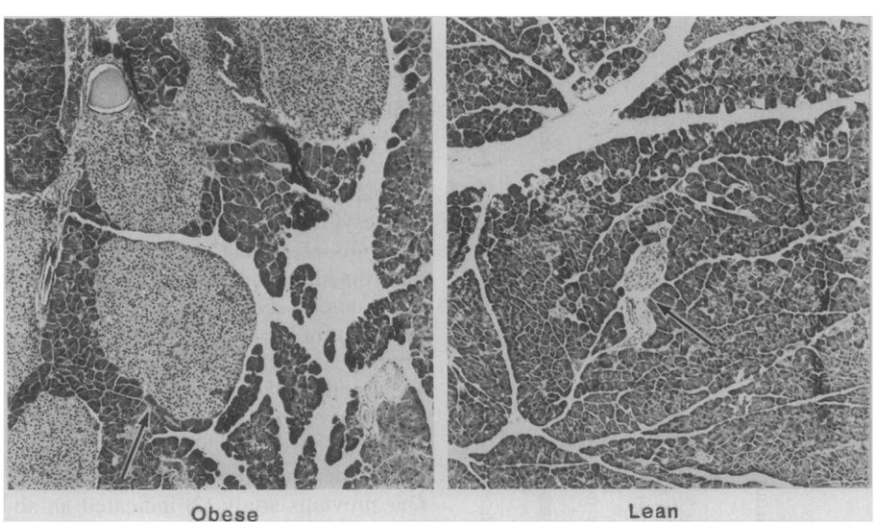

Fig. 3. Section of pancreas from obese mouse, showing marked hyperplasia in islet tissue, and section from pancreas of lean littermate. Arrows indicate islet tissue.

Nevertheless, a central lesion could be of pivotal importance in the development of the syndrome. To evaluate this, we analyzed brain catecholamines in the mice. Catecholamines have been implicated in abnormal endocrine function in *ob/ob* mice (*8*) and probably are important in hypothalamic control of feeding patterns (*9*). Catecholamine levels were determined in the brainstem, hypothalamus, and forebrain of five obese animals, five infected lean controls, and five uninfected lean controls by the analytical procedure of Hegstrand and Eichelman (*10*), which involves high-pressure liquid chromatography with electrochemical detection. Concentrations of dopamine and norepinephrine in forebrain specimens from obese animals were two to three times lower than in specimens from uninfected lean controls. Forebrain from infected lean controls had concentrations of dopamine and norepinephrine that were intermediate between those measured in forebrain from obese and uninfected controls. Catecholamine levels in hypothalamic specimens from infected animals, both lean and obese, were difficult to evaluate because of considerable variance. There were no significant differences in brainstem dopamine and norepinephrine between obese mice, infected lean controls, and uninfected lean controls. Thus a primary pathological process involving virus-induced destruction (or dysfunction) of select groups of neurons, resulting in defective catecholamine synthesis or release, may be critical in the development of the syndrome. Studies of a variety of other physiological and biochemical variables are needed to fully describe this type of obesity.

There is a clear role for virus infection in the initiation of a number of chronic disorders in man (*11*). The present findings raise the possibility that virus infection also plays a role in some cases of obesity in children and in some cases of severe spontaneous obesity in adults.

MICHAEL J. LYONS
IRVING M. FAUST
RICHARD B. HEMMES
DANIEL R. BUSKIRK
JULES HIRSCH
JOHN B. ZABRISKIE
Rockefeller University, New York 10021

References and Notes

1. P. R. Johnson and J. Hirsch, *J. Lipid Res.* **13**, 2 (1972).
2. M. J. Lyons, W. W. Hall, C. Petito, V. Cam, J. B. Zabriskie, *Neurology* **30**, 92 (1980).
3. I. M. Faust, P. R. Johnson, J. Hirsch, *Am J. Physiol.* **231**, 538 (1976); J. Hirsch and E. Gallian, *J. Lipid Res.* **10**, 77 (1969).
4. C. Orvell and E. Norrby, *J. Immunol.* **113**, 1850 (1950); W. W. Hall, R. A. Lamb, P. W. Choppin, *Virology* **100**, 433 (1980).
5. I. M. Faust, P. R. Johnson, J. S. Stern, J. Hirsch, *Am. J. Physiol.* **235**, E279 (1978).
6. S. K. Gale, T. B. Van Itallie, I. M. Faust, *Metabolism* **30**, 105 (1981); J. S. Stern and R. E. Keesey, *Nutr. Rep. Int.* **23**, 295 (1981).
7. J. Hirsch and P. W. Han, *J. Lipid Res.* **10**, 77 (1969).
8. J. F. Lorden, G. A. Oltmans, D. L. Margules, *Brain Res.* **96**, 390 (1975).
9. J. B. Martin, S. Reichlin, G. M. Brown, *Clinical Neuroendocrinology* (Davis, Philadelphia, 1977); S. F. Leibowitz, in *Handbook of Hypothalamus*, P. J. Morgane and J. Panksepp, Eds. (Dekker, New York, 1980), vol. 3, pp. 299–437.
10. L. R. Hegstrand and B. Eichelmen, *J. Chromatogr.* **222**, 107 (1981).
11. J.-W. Yoon, M. Austin, T. Onodera, A. B. Notkins, *N. Engl. J. Med.* **300**, 1173 (1979); J. E. Craighead, *Am. J. Med.* **70**, 127 (1981); L. Horta-Barbosa, D. A. Fuccillo, J. L. Sever, W. Zeman, *Nature (London)* **221**, 974 (1969); F. E. Payne, J. V. Baublis, H. H. Itabashi, *N. Engl. J. Med.* **281**, 585 (1969); J. F. Woodruff, *Am. J. Pathol.* **101**, 427 (1980).
12. We thank C. Petito and J. Walberg for performing histopathological examinations. Supported in part by National Multiple Sclerosis Society grant RG794-C-3, National Institutes of Health grant AM 20508, and the Howard M. Pack Foundation.

26 August 1981; revised 18 December 1981

Dynorphin and Vasopressin: Common Localization in Magnocellular Neurons

Abstract. *The opioid peptide dynorphin is widely distributed in neuronal tissue of rats. By immunocytochemical methods, it was shown previously that dynorphin-like immunoreactivity is present in the posterior pituitary and the cells of the hypothalamic neurosecretory magnocellular nuclei which also are responsible for the synthesis of oxytocin, vasopressin, and their neurophysins. By using an affinity-purified antiserum to the non-enkephalin part of the dynorphin molecule it has now been demonstrated that dynorphin and vasopressin occur in the same hypothalamic cells of rats, whereas dynorphin and oxytocin occur in separate cells. Homozygous Brattleboro rats (deficient in vasopressin) have magnocellular neurons that contain dynorphin separate from oxytocin. Thus dynorphin and vasopressin, although they occur in the same cells, appear to be under separate genetic control and presumably arise from different precursors.*

The opioid peptide dynorphin, which was originally extracted from porcine pituitary, is highly active in the guinea pig ileum bioassay for opiate activity (700 times more potent than leucine-enkephalin) (*1*). By radioimmunoassay dynorphin has been demonstrated in the neurointermediate lobe of the pituitary, hypothalamus, cortex, hippocampus, medulla-pons, spinal cord, and dorsal-root ganglia of rats (*2, 3*). We previously demonstrated that immunoreactive dynorphin occurs in cells other than β-endorphin–producing cells and pituitary in rat brain (*4*). We located dynorphin in the posterior pituitary and the magnocellular nuclei of the hypothalamus (supraoptic and paraventricular nuclei). Since the magnocellular components of these nuclei are associated with the production of oxytocin, vasopressin, and the enkephalins (*5*), we undertook an anatomical study of the cellular distribution of dynorphin and these peptides. We now report the presence of immunoreactive dynorphin in cells that produce vasopressin. We also show that Brattleboro rats, known to be deficient in the production of vasopressin and its neurophysin (*6*), contain dynorphin in the non-oxytocin–containing cells of the magnocellular nuclei. This, along with a 300-fold difference in content of arginine vasopressin (AVP) and dynorphin (*2, 7*) suggests that the peptides are under different biosynthetic control.

Brain tissue was prepared from Sprague-Dawley rats for immunocytochemical study as reported elsewhere (*4*). In brief, normal rats and rats treated with colchicine (50 μg/50 μl, injected into the cerebral ventricles 48 hours before the rats were killed) were anesthetized with pentobarbital (50 mg/kg) and perfused by way of the aorta with 4 percent cold formaldehyde phosphate buffer (0.1*M*) at 4°C for 30 minutes. The brains were removed, blocked, and post-fixed in the same fixative and maintained overnight at 4°C in 0.1*M* phosphate-buffered normal saline, *p*H 7.2, with 15 percent sucrose. They were then frozen in liquid nitrogen and sectioned at −20°C on a cryostat. Serial 5-μm sections were cut through the hypothalamic magnocellular nuclei.

Immunocytochemical staining was carried out according to the PAP technique (*8*) with antiserums to dynorphin-(1–13), AVP, and oxytocin. Dynorphin-(1–13) was conjugated via glutaraldehyde to thyroglobulin as reported (*2*). To reduce nonspecific background reactivity in the immunocytochemical study we used affinity-purified and fully recharacterized dynorphin antibodies. The affinity resin used for antibody purification was prepared by linking dynorphin(1–13) to cyanogen bromide–activated Sepharose 4B with cyanogen bromide (*9*). The resulting antibodies were used at a 1/300 dilution; they were found to be blocked

0036-8075/82/0402-0085$01.00/0